The critical closing pressure contribution to dynamic cerebral autoregulation in humans: influence of arterial partial pressure of CO_2

Ronney B. Panerai[1,2], Jatinder S. Minhas[1,2] (iD), Osian Llwyd[1], Angela S. M. Salinet[3], Emmanuel Katsogridakis[4], Paola Maggio[5] (iD) and Thompson G Robinson[1,2]

[1]*Cerebral Haemodynamics in Ageing and Stroke Medicine (CHiASM) Research Group, Department of Cardiovascular Sciences, University of Leicester, Leicester, UK*

[2]*NIHR Leicester Biomedical Research Centre, British Heart Foundation Cardiovascular Research Centre, Glenfield Hospital, Leicester, UK*

[3]*Neurology Department, Hospital das Clinicas, School of Medicine, University of Sao Paulo, Sao Paulo, Brazil*

[4]*Department of Vascular Surgery, Wythenshawe Hospital, Manchester Foundation Trust, Manchester, UK*

[5]*Neurology Department, ASST Bergamo EST (BG), Italy*

Key points

- Dynamic cerebral autoregulation (CA) is often expressed by the mean arterial blood pressure (MAP)–cerebral blood flow (CBF) relationship, with little attention given to the dynamic relationship between MAP and cerebrovascular resistance (CVR).
- In CBF velocity (CBFV) recordings with transcranial Doppler, evidence demonstrates that CVR should be replaced by a combination of a resistance–area product (RAP) with a critical closing pressure (CrCP) parameter, the blood pressure value where CBFV reaches zero due to vessels collapsing.
- Transfer function analysis of the MAP–CBFV relationship can be extended to the MAP–RAP and MAP–CrCP relationships, to assess their contribution to the dynamic CA response.
- During normocapnia, both RAP and CrCP make a significant contribution to explaining the MAP–CBFV relationship.
- Hypercapnia, a surrogate state of depressed CA, leads to marked changes in dynamic CA, that are entirely explained by the CrCP response, without further contribution from RAP in comparison with normocapnia.

Abstract Dynamic cerebral autoregulation (CA) is manifested by changes in the diameter of intra-cerebral vessels, which control cerebrovascular resistance (CVR). We investigated the contribution of critical closing pressure (CrCP), an important determinant of CVR, to explain the cerebral blood flow (CBF) response to a sudden change in mean arterial blood pressure (MAP). In 76 healthy subjects (age range 21–70 years, 36 women), recordings of MAP (Finometer), CBF

Ronney B. Panerai is an Emeritus Professor, Department of Cardiovascular Sciences, University of Leicester and Leicester NIHR Biomedical Research Centre in Cardiovascular Disease, Glenfield Hospital, Leicester, UK. His main research interests are in physiological measurement and modelling, particularly in physiological and clinical studies of cerebral blood flow regulation.

---

velocity (CBFV; transcranial Doppler ultrasound), end-tidal CO_2 (capnography) and heart rate (ECG) were performed for 5 min at rest (normocapnia) and during hypercapnia induced by breathing 5% CO_2 in air. CrCP and the resistance–area product (RAP) were obtained for each cardiac cycle and their dynamic response to a step change in MAP was calculated by means of transfer function analysis. The recovery of the CBFV response, following a step change in MAP, was mainly due to the contribution of RAP during both breathing conditions. However, CrCP made a highly significant contribution during normocapnia ($P < 0.0001$) and was the sole determinant of changes in the CBFV response, resulting from hypercapnia, which led to a reduction in the autoregulation index from 5.70 ± 1.58 (normocapnia) to 4.14 ± 2.05 (hypercapnia; $P < 0.0001$). In conclusion, CrCP makes a very significant contribution to the dynamic CBFV response to changes in MAP and plays a major role in explaining the deterioration of dynamic CA induced by hypercapnia. Further studies are needed to assess the relevance of CrCP contribution in physiological and clinical studies.

Corresponding author R. B. Panerai: Department of Cardiovascular Sciences, University of Leicester, Sir Robert Kilpatrick Clinical Sciences Building, Leicester Royal Infirmary, Leicester LE2 7LX, UK.   Email: rp9@le.ac.uk

Introduction

In healthy individuals, rapid changes in mean arterial blood pressure (MAP) induce corresponding changes in cerebral blood flow (CBF), which subsequently return to original levels, within a few seconds, a phenomenon that has been termed *dynamic cerebral autoregulation* (CA) (Aaslid *et al.* 1989). This response of CBF to changes in MAP is predominantly controlled by myogenic mechanisms (Faraci *et al.* 1989), with the probable additional involvement of metabolic control (Willie *et al.* 2014), as expressed by the strong influence of arterial CO_2 (P_{aCO_2}) on the efficiency of dynamic CA (Aaslid *et al.* 1989; Murkin, 2007; Hoiland *et al.* 2019). Both myogenic and metabolic pathways lead to alterations in vascular smooth muscle (VSM) contractility, with consequent changes in the diameter of intra-cerebral arteries, which will then control CBF due to corresponding changes in cerebrovascular resistance (CVR). By far, most physiological and clinical studies of dynamic CA have focused on the dynamic relationship between MAP and CBF (Panerai, 1998; van Beek *et al.* 2008; Czosnyka *et al.* 2009; Claassen *et al.* 2016), with only a few studies reporting on the temporal changes in CVR that ultimately determine the CBF response (Aaslid *et al.* 1989; Garnham *et al.* 1999; Hughson *et al.* 2001; Edwards *et al.* 2002; O'Leary *et al.* 2004; Panerai *et al.* 2006). However, a major limitation of these studies exists: adopting the definition of CVR as the ratio of MAP/CBF (or CBF velocity (CBFV), given the dominant use of transcranial Doppler ultrasound in these studies), there is the inherent assumption that the instantaneous pressure–velocity relationship passes through the origin. In other words, according to this formula, CBF becomes zero only when MAP = 0. However, the overwhelming evidence is that, similar to the lung (Burton, 1951), the cerebral circulation also shows the existence of a *critical closing pressure* (CrCP), whereby CBF stops at blood pressure values significantly greater than zero (Panerai, 2003). As modelled by Burton (1951), CrCP is likely to result from the balance between transmural pressure, hence reflecting the influence of intracranial pressure (ICP), and arterial wall tension, which would depend on vessel diameter, VSM tone and its activation (Burton, 1951). In fact, CrCP has been shown to be highly sensitive to changes in P_{aCO_2} (Panerai, 2003), and it has been suggested that it could show a greater association to metabolic mechanisms of VSM contraction, as distinct from myogenic control (Panerai *et al.* 2005; Panerai *et al.* 2012). Accepting that CrCP > 0, a more realistic model of the pressure–flow (or velocity) relationship would be CBFV = (MAP − CrCP)/RAP, where RAP is the resistance–area product. RAP represents the slope of the instantaneous pressure–velocity relationship and takes into account that mean cross-sectional blood velocity is the absolute flow divided by arterial cross-sectional area (Evans *et al.* 1988).

The distinct contributions of CrCP and RAP to the dynamic CBFV response to changes in MAP have been reported in previous physiological (Maggio *et al.* 2013) and clinical studies, including for conditions such as stroke (Salinet *et al.* 2013), autonomic dysfunction (Castro *et al.* 2014) and pre-eclampsia (van Veen *et al.* 2015). For this purpose, one attractive approach is *sub-component analysis*, whereby any changes in CBFV can be broken down into the separate contributions of MAP, CrCP and RAP (Panerai *et al.* 2005). In the present study, we have merged this approach with the estimation of the CBFV response to a step change in MAP, as one of the conventional techniques that is often adopted for assessment of dynamic CA (Panerai *et al.* 2001). The CBFV step response approach is intrinsically linked to the autoregulation index (ARI), proposed by Tiecks *et al.* (1995),

in the form of 10 template curves that represent values of ARI ranging from zero (absence of CA) to 9 (best observed CA). We and others have obtained estimates of the CBFV step response using frequency- or time-domain techniques to model the dynamic MAP–CBFV relationship (Panerai *et al.* 1998*b*; Edwards *et al.* 2004; Liu *et al.* 2005; Elting *et al.* 2014; Marmarelis *et al.* 2014) from which values of ARI can be obtained by comparison with the Tiecks template curve providing the best match (Panerai *et al.* 1998*b*). Step responses have been reported for CVR (Edwards *et al.* 2004) and RAP (Panerai *et al.* 2006), but not for CrCP. Given the relevance of RAP and CrCP as determinants of the instantaneous blood pressure (BP)–CBFV relationship in each cardiac cycle, further investigations are needed on their contribution to the regulation of CBF, particularly their role in the dynamic response of CBF to rapid changes in MAP. In this study, we used sub-component analysis to obtain separate estimates of CBFV, RAP and CrCP step responses to changes in MAP in healthy subjects, during normocapnia and hypercapnia, to test two interrelated hypotheses. First, that during normocapnia CrCP makes a significant contribution to the dynamic CA response to sudden changes in MAP. Second, that during hypercapnia, a surrogate state for impairment of dynamic CA, the CrCP step response is the dominant sub-component to explain the deterioration in CA induced by breathing 5% CO_2 in air.

Methods

Ethical approval

All studies were approved by the UK Research Ethics Committees from Southampton and South West Hampshire (10/H0502/1), Nottingham (11/EM/0016), North East-Newcastle and North Tyneside (14/NE/1003) and the University of Leicester (jm591-c033). All procedures were conducted in accordance with the *Declaration of Helsinki* and all participants provided written informed consent.

Subjects and measurements

The study re-analysed recordings performed in healthy subjects, included in the Leicester database (Patel *et al.* 2016), who underwent measurements during normocapnia and hypercapnia, induced by breathing 5% CO_2 in air (Katsogridakis *et al.* 2013; Maggio *et al.* 2013; Llwyd *et al.* 2017; Minhas *et al.* 2018a). Subjects were 18 years of age or older without any history or symptoms of cardiovascular, neurological or respiratory disease.

Recordings were performed at the University of Leicester's Cerebral Haemodynamics in Ageing and Stroke

Medicine (CHIASM) research laboratory, which was maintained at controlled temperature (20–23°C) and with minimal auditory or visual distraction. Volunteers were asked to avoid heavy exercise, caffeine, alcohol and nicotine for at least 4 h prior to measurements. CBFV was measured in both middle cerebral arteries (MCAs) using transcranial Doppler ultrasound (TCD; Vyasis Companion III, Vyasis Healthcare, Hochberg, Germany) with 2 MHz probes secured in place using a head-frame. End-tidal CO_2 (ET_{CO_2}) was recorded continuously via nasal prongs (Salter Labs, Lake Forest, IL, USA) or a face mask, by a capnograph (Capnocheck Plus, Smiths Medical ASD, Inc., Norwell, MA, USA). Heart rate was derived from a three-lead electrocardiogram (ECG). BP was recorded continuously using a Finapres/Finometer device (FMS, Finapres Measurement Systems, Arnhem, Netherlands), attached to the middle finger of the left hand. Systolic and diastolic BP were measured by classical brachial sphygmomanometry before each 5 min recording. The servo-correcting mechanism of the Finapres/Finometer was switched on and then off prior to measurements.

Data were simultaneously recorded onto a data acquisition system (PHYSIDAS, Department of Medical Physics, University Hospitals of Leicester, Leicester, UK) for subsequent off-line analysis using a sampling rate of 500 samples/s.

Experimental protocol

All recordings followed a similar protocol and were performed by investigators trained to rigorous standard procedures. After resting for 20 min in the supine position with the head elevated at 30°, two 5 min recordings were performed in each subject. The first recording corresponded to baseline resting conditions with subjects breathing ambient air. In the second recording, after a 60 s period of breathing air, subjects were switched to breathing 5% CO_2 in air, through a face mask that was tightly fitted to avoid leakage, as confirmed by visual inspection of the end-tidal CO_2 waveform. After 3 min of CO_2 breathing, subjects were returned to ambient air and a further 60 s was recorded during return to normocapnia.

Data analysis

All signals were visually inspected to identify artefacts; noise and narrow spikes (<100 ms) were removed by linear interpolation. CBFV channels were subjected to a median filter and all signals were low-pass filtered with a eighth order Butterworth filter with cut-off frequency of 20 Hz. BP was calibrated at the start of each recording using systolic and diastolic values obtained with sphygmomanometry. The R–R interval was then automatically marked from the ECG and beat-to-beat

heart rate (HR) was plotted against time. Occasional missed marks caused spikes in the HR signal; these were manually removed by remarking the R–R intervals for the time points at which they occurred. Mean, systolic and diastolic BP and CBFV values were calculated for each cardiac cycle. CrCP and RAP were calculated using the first harmonic method (Panerai *et al.* 2011). The end of each expiratory phase was detected in the ET_{CO_2} signal, linearly interpolated and resampled with each cardiac cycle. Beat-to-beat data were spline interpolated and resampled at five samples/s to produce signals with a uniform time base.

Transfer function analysis (TFA) of the MAP–CBFV relationship was performed using Welch's method (Welch, 1967) with data segmented with 102.4 s duration and 50% superposition (Claassen *et al.* 2016). The mean values of MAP and CBFV were removed from each segment and a cosine window was applied to minimise spectral leakage. The squared coherence function, gain and phase frequency responses were calculated from the smoothed auto- and cross-spectra using standard procedures (Panerai *et al.* 1998*a*; Claassen *et al.* 2016). The CBFV step response to the MAP input was estimated using the inverse fast Fourier transform of gain and phase (Bendat & Piersol, 1986). ARI, which represents dynamic CA, was extracted by using the normalised minimum square error (NMSE) fit between the CBFV step response and one of the 10 model ARI curves proposed by Tiecks *et al.* (1995). ARI values were only accepted if the mean squared coherence function for the 0.15–0.25 Hz frequency interval was above its 95% confidence limit, adjusted for the corresponding degrees of freedom, and the NMSE was ≤0.30 (Panerai *et al.* 2016).

Sub-component analysis. As detailed in the Appendix, the relationship between mean CBFV, MAP, CrCP and RAP for each cardiac cycle can be expressed as a function of three distinct sub-components, representing the different contributions to a change in CBFV, that is:

$$V_{MCA} = V_{MAP} + V_{CrCP} + V_{RAP}.$$

When this expression is normalised as a percentage, the total percent change in V_{MCA} can then be explained by the corresponding sum of the percent changes in the sub-components, that is V_{MAP}, V_{CrCP} and V_{RAP} (Appendix). For normalisation as a percentage, and also to obtain the beat-to-beat differences from the mean (Δv, Δp, Δc, Δr; eqn (A3)), the mean values of CBFV, MAP, CrCP and RAP were obtained for the entire duration of each 5 min segment of data.

In the above expression for V_{MCA}, if V_{MAP} changes suddenly, as a perfect step function, the resulting changes in V_{MCA}, V_{CrCP} and V_{RAP} will be the corresponding step responses for the V_{MAP} input. Each of these three-step responses were derived by TFA, as described above for the

CBFV–MAP relationship, and from the above expression it is possible to write:

$$SRV^*_{MAP} = SRV_{MCA} - SRV_{CrCP} - SRV_{RAP}$$

where SRV^*_{MAP} is an estimate of the MAP step change, based on the summation of the three other step responses (SR). Therefore, the expression above works as a 'checksum' for the correctness of the three distinct SR estimated for V_{MCA}, V_{CrCP} and V_{RAP}.

Statistical analysis

As explained above, SRV_{MCA} was only accepted based on the dual criteria of coherence above the 95% confidence limit and a NMSE ≤0.30 for fitting of the Tiecks model (Tiecks *et al.* 1995; Panerai *et al.* 2016). For reasons that will be discussed later, SRV_{CrCP} and SRV_{RAP} were only accepted if their corresponding transfer functions both had mean coherence above the 90% confidence limit (in the 0.15–0.25 Hz range), for at least one of the hemispheres, assuming that SRV_{MCA} had also been accepted, for both normocapnia and hypercapnia. In other words, for the right or left hemisphere to be accepted, all three-step responses for that hemisphere had to be accepted for both normocapnia and hypercapnia.

With the exception of the mean coherence, all other parameters were treated as normally distributed (Patel *et al.* 2016). The distribution of coherence was expressed by its median (interquartile limits), all other parameters as the mean ± SD. Differences between parameters were assessed using the paired Student's *t* test or the Wilcoxon test. In each of the SR, values were averaged for three distinct time intervals; T1 (0.6–1.4 s), T2 (3–4 s) and T3 (7–10 s). T1 corresponds to the peak of the SRV_{MCA}, T2 the beginning of its plateau phase, and T3 the tail of the response (Figs 1*A* and 2*A*). Differences in SR values from T1 to T2 and then at T3 were used with repeated measures ANOVA to test the effects of breathing condition (normocapnia *vs.* hypercapnia) and relative contribution of each SR to explain the V_{MCA} change. SRs and ARI values were averaged for the right and left hemispheres when both were accepted. A *P*-value of <0.05 was adopted to indicate statistical significance.

Results

A total of 120 good quality recordings were extracted from the database for healthy subjects with measurements of CBFV, BP and ET_{CO_2} for both normocapnia and hypercapnia. Forty-four subjects were rejected as the strict conditions imposed for acceptance of all three SR were not met by either hemisphere, for both normocapnia and hypercapnia. The remaining 76 subjects (36 women) had mean ± SD age 43.3 ± 13.8 years, range 21–70 years.

In six of these subjects, CBFV was not recorded in the left MCA. Hypercapnia induced changes in CBFV, mean and diastolic BP, heart rate and mean CrCP (Table 1), but did not affect mean RAP in either hemisphere.

The average coherence in the frequency range 0.15–0.25 Hz for the V_{MAP}–V_{MCA} transfer function for both normocapnia (0.74 (0.58, 0.85)) and hypercania (0.76 (0.55, 0.86)) was higher than corresponding values for the V_{MAP}–V_{RAP} (0.23 (0.18, 0.33); 0.26 (0.19, 0.32)) and V_{MAP}–V_{CrCP} (0.29 (0.21, 0.39); 0.29 (0.22, 0.39)) transfer functions, respectively.

Figure 1 presents the SRV_{MCA}, SRV_{RAP} and SRV_{CrCP} for a representative subject with corresponding population averages given in Fig. 2. Noteworthily, Fig. 1D demonstrates that the 'checksum' for SRV_{MAP} yields a temporal pattern that confirms the correctness of the three other SRs that were calculated independently. A similar result was obtained for all subjects.

Following the step change in V_{MAP}, SRV_{MCA} showed a sudden change, followed by a relatively rapid recovery towards baseline values, which was more pronounced during normocapnia as compared to hypercapnia (Figs 1A and 2A; $P < 0.0001$). The effects of hypercapnia were also reflected by the ARI, corresponding to 5.70 ± 1.58 and 4.14 ± 2.05 ($P < 0.0001$) for normocapnia and hypercapnia, respectively. The negative temporal pattern of the SRV_{RAP} (Figs 1B and 2B) reflects its relevant contribution to the reduction of the SRV_{MCA}, without a difference between normocapnia and hypercapnia. V_{CrCP} presented a more complex step response (Figs 1C and 2C), undergoing a dip around 2–3 s after the V_{MAP} step change, followed by a slow recovery, which was more pronounced during hypercapnia ($P < 0.0001$). Due to this biphasic pattern, SRV_{CrCP} initially contributed to reduce SRV_{MCA}, but after 5–6 s it tended to increase SRV_{MCA}. After reaching a peak around $t = 1$ s, SRV_{MCA} showed a sharp drop, up until around $t = 3$ s, due to an active CA (Figs 1A and 2A). On average, this drop was approximately 59% for normocapnia and 39% for hypercapnia, and it was dominated by the SRV_{RAP} contribution (Table 2). Noteworthily, SRV_{CrCP} had a highly significant contribution during both normocapnia and hypercapnia to explain the overall SRV_{MCA} variance (Table 2, $P < 0.0001$).
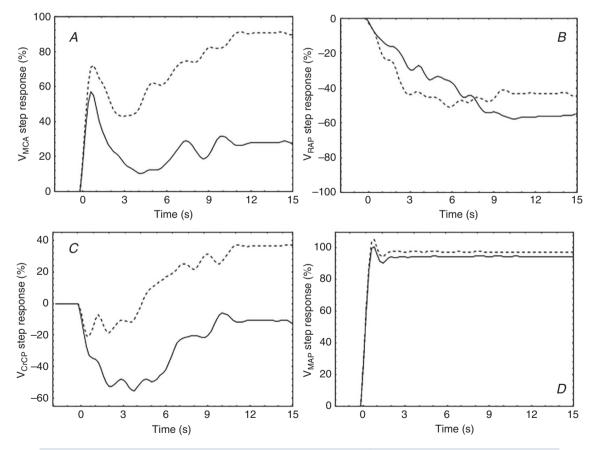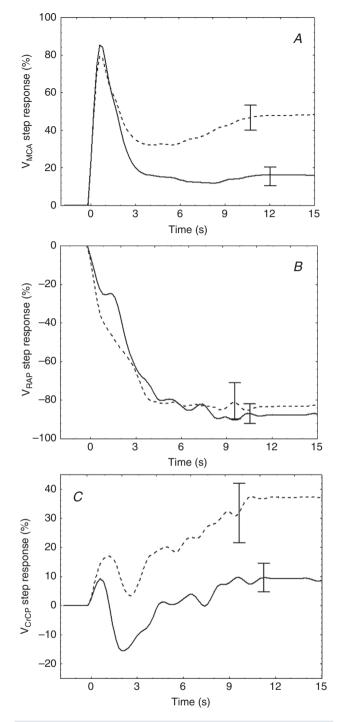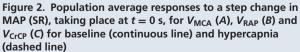

Figure 1. Representative step responses from a 40-year-old female subject during normocapnia (continuous line) and hypercapnia (dashed line)
A, V_{MCA} step response for MAP input; *B*, V_{RAP} step response for MAP input; *C*, V_{CrCP} step response for the MAP input; *D*, V_{MAP} step changes, reconstructed from the sum of the three step responses in *A–C*. The overshoot at the start of the response is due to the smoothing of spectral estimates with Welch's method.

Figure 2. Population average responses to a step change in MAP (SR), taking place at $t = 0$ s, for V_{MCA} (*A*), V_{RAP} (*B*) and V_{CrCP} (*C*) for baseline (continuous line) and hypercapnia (dashed line)

The error bars represent the largest ± 1 SEM at the point of occurrence.

Table 1. Distribution of physiological parameters during normocapnia and hypercapnia

Parameter	Normocapnia	Hypercapnia	*P*
Systolic BP (mmHg)	128.0 ± 23.3	131.7 ± 25.8	0.065
Mean BP (mmHg)	90.1 ± 15.3	92.8 ± 16.7	0.023
Diastolic BP (mmHg)	72.4 ± 13.2	74.7 ± 14.2	0.018
$CBFV_R$ (cm s^{-1})	55.1 ± 12.6	65.4 ± 17.8	<0.0001
$CBFV_L$ (cm s^{-1}) ($n = 70$)	53.1 ± 12.2	63.6 ± 19.8	<0.0001
End-tidal CO_2 (mmHg)	39.8 ± 2.6	45.4 ± 3.6	<0.0001
Heart rate (bpm)	67.7 ± 10.7	68.7 ± 10.8	0.017
$CrCP_R$ (mmHg)	33.4 ± 13.6	30.1 ± 13.6	0.010
$CrCP_L$ (mmHg) ($n = 70$)	33.3 ± 14.0	30.5 ± 13.3	0.037
RAP_R (mmHg s cm^{-1})	1.17 ± 0.44	1.11 ± 0.44	0.17
RAP_L (mmHg s cm^{-1}) ($n = 70$)	1.16 ± 0.44	1.09 ± 0.45	0.078

Values are means $\pm$ SD for $n = 76$ subjects, unless specified, averaged for the entire 5 min recording. *P*-values for paired *t* tests between normocapnia and hypercapnia. BP, blood pressure; CBFV, cerebral blood flow velocity; CrCP, critical closing pressure; RAP, resistance–area product; R/L, right/left MCA.

Table 2. Change in step responses (SR) of sub-components during CBFV recovery phase (1–3 s) for both normocapnia and hypercapnia

Step response change	Normocapnia	Hypercapnia
$\triangle SRV_{MCA}$ (%)	58.77 ± 10.97	39.08 ± 20.41
$\triangle SRV_{RAP}$ (%)	43.23 ± 31.35	33.70 ± 26.86
$\triangle SRV_{CrCP}$ (%)	$15.00 \pm 30.69^*$	$4.41 \pm 27.61^*$

$^*P < 0.0001$ for contribution of $\triangle SRV_{CRCP}$ to explain $\triangle SRV_{MCA}$ change. CBFV, cerebral blood flow velocity; CrCP, critical closing pressure; RAP, resistance–area product; $\triangle SRV_{CrCP}$, SRV_{MCA} change due to CrCP; $\triangle SRV_{MCA}$, total SRV_{MCA} change; $\triangle SRV_{RAP}$, SRV_{MCA} change due to RAP subcomponent.

At a later stage of the response ($t > 7$ s), the two-way ANOVA indicated that the differences in SRV_{MCA} between normocapnia and hypercapnia were solely due to SRV_{CrCP} ($P < 0.0001$), without a contribution from SRV_{RAP} (Fig. 3).

Of note, *a posteriori* analysis of the data, for $n = 120$ subjects, thus including the 44 subjects that were removed due to low TFA coherence, did not show any significant differences in comparison with the results in Figs 2 and 3 and Tables 1 and 2 (results not shown).

Discussion

In the brain, as well as in several other organs, reductions in transmural pressure can lead to the collapse of small vessels, resulting in the cessation of blood flow, thus defining the critical closing pressure of each particular circulation (Burton, 1951; Garnham *et al.* 1999; Panerai, 2003; Panerai *et al.* 2005, 2011; Varsos *et al.* 2013; Castro

et al. 2014; Minhas *et al.* 2018*a*, 2019). Despite evidence that CrCP and RAP, the slope of the instantaneous relationship between MAP and CBFV, might make distinct contributions to the regulation of CBF (Panerai *et al.* 2012), the role of CrCP in dynamic CA, as expressed by the temporal response of CBF (or CBFV) to rapid changes in MAP, has been largely ignored. Based on a relatively large group of healthy individuals, we have demonstrated that CrCP and RAP make significant, albeit distinct, contributions to the dynamic CA response, with the corollary that it is the CrCP response, and not the RAP, that explains the depression in dynamic CA efficiency observed during hypercapnia.
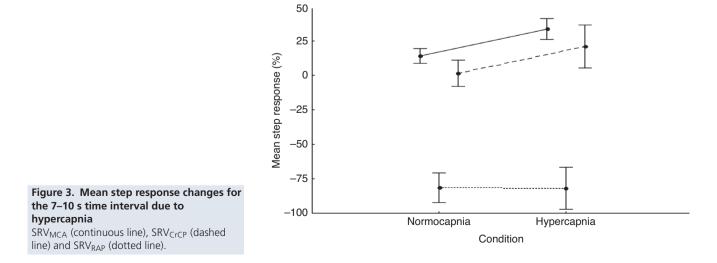
Main findings

Sub-component analysis (SCA) expresses changes in CBFV (V_{MCA}) broken down into the separate contributions of MAP (V_{MAP}), RAP (V_{RAP}) and CrCP (V_{CrCP}) (Panerai *et al.* 2005). Due to the linearity of transfer function analysis, a step change can also be parcelled out into the sum of the corresponding distinct SRs, as demonstrated by the 'checksum' in the Methods and Appendix, and in Fig. 1*D*. Our findings agreed with the temporal pattern of the SRV_{MCA}, described in several previous studies (Panerai *et al.* 2006, 2016) and its changes due to hypercapnia (Panerai *et al.* 1999; Katsogridakis *et al.* 2013). We have also confirmed that the temporal pattern of the SRV_{RAP} tends to follow a gradual change, similar to an exponential curve, which was reported in a few studies (Panerai *et al.* 2006, 2011), with a pattern similar to that described for the CVR step response as well (Edwards *et al.* 2004). Of note, when the RAP or CVR step responses are calculated using standard units, the resulting curves tend to rise continually, as expected from the myogenic response, leading to a corresponding reduction in CBF. With the SCA method, though, V_{RAP} is

expressed in units of flow/velocity, with the negative sign in eqn (A9) meaning that vasoconstriction will lead to a reduction in V_{RAP}, with consequent reductions in CBFV. For this reason, the SRV_{RAP} showed the negative curves displayed in Figs 1*B* and 2*B*.

Our main novel finding, though, was that the SRV_{CrCP} made a highly significant contribution to explaining the V_{MCA} changes in response to a step change in V_{MAP}, and that it was solely responsible for explaining the changes in SRV_{MCA} during hypercapnia. Taken together, these two original findings lead to the acceptance of our two main hypotheses, and should have considerable impact on our understanding of the dynamic CA response in humans. As discussed below, including the role of V_{CrCP} in future investigations could represent a paradigm shift in our ability to progress towards a more detailed assessment of dynamic CA in physiological and clinical studies.

Methodological considerations

Similarly to ARI (Tiecks *et al.* 1995), the majority of indices proposed for assessment of dynamic CA are encapsulated in a single number, such as the rate of regulation (RoR) (Aaslid *et al.* 1989), the mean flow index (Mx) (Czosnyka *et al.* 1996) or the pressure–reactivity index (PRx) (Czosnyka *et al.* 1997). Although expressing the effectiveness of CA with a single number is convenient, mainly in clinical applications, it is unlikely that the complexity of the multiple mechanisms underlying the CA response can be reduced to a unidimensional entity. In TFA of the dynamic relationship between MAP and CBFV, theoretical considerations would indicate that each harmonic of the gain and phase frequency responses behaves as a statistical independent quantity, which could offer the possibility of overcoming the dimensional limitations of other indices. However, despite an extensive literature on the application of TFA to

Figure 3. Mean step response changes for the 7–10 s time interval due to hypercapnia
SRV_{MCA} (continuous line), SRV_{CrCP} (dashed line) and SRV_{RAP} (dotted line).

physiological and clinical studies, segmentation of the spectral range where dynamic CA is active, from DC to approximately 0.2 Hz (Panerai *et al.* 2019), into averages over the very low and low frequency ranges (Zhang *et al.* 1998; Claassen *et al.* 2016) has not led to consistent metrics that could be treated as independent indicators in different physiological conditions, or reflecting specific pathophysiological alterations in different cerebrovascular conditions (Panerai, 2008; Tzeng *et al.* 2012; Intharakham *et al.* 2019). To our knowledge, the demonstration that SRV_{CrCP} makes a significant contribution to the dynamic CA response, and can explain the differences in SRV_{MCA} due to hypercapnia, is the first evidence that it should be possible to quantify the phenomenon of dynamic CA in more than a single dimension. Further physiological and clinical studies are needed, though, to confirm whether the additional information that could be obtained with the joint use of SRV_{CrCP} and SRV_{RAP} allows greater understanding of the behaviour of CA in different phenotypes, physiological conditions or in cerebrovascular diseases of different aetiology. From a methodological perspective, it would also be useful to advance mathematical models, similar to the one proposed by Tiecks *et al.* for ARI (Tiecks *et al.* 1995), that would allow further quantification of the SRV_{CrCP} and SRV_{RAP}.

Despite the promising possibilities offered by our preliminary findings, a word of caution is needed, given the limitations involved in the calculation of CrCP and RAP for each cardiac cycle. Non-invasive BP was measured in the finger and CBFV in the MCA. Due to the time delay in BP wave propagation, when CBFV is plotted as a function of BP for each cardiac cycle, the resulting graph shows a loop, instead of the linear relationship implied by eqn (A1). For this reason, before applying methods like linear regression analysis to estimate the CrCP and RAP parameters, the CBFV and BP waveforms need to be shifted in time, which normally yields a more linear relationship (Panerai, 2003). The first harmonic method to obtain estimates of RAP and CrCP that we adopted (Panerai *et al.* 2011) has the advantage of not needing compensation for the propagation time delay, but could still be affected by differences in BP waveform morphology between the finger and the MCA. These factors could be behind the much poorer signal-to-noise ratios that are often observed in time series of beat-to-beat estimates of CrCP and RAP, which were likely to have caused the low values of coherence that led to the rejection of 44 subjects in our study. With the inherent difficulty of obtaining good quality recordings in clinical settings, it is possible that an even larger fraction of patients could not provide suitable data for acceptable estimates of SRV_{CrCP} and SRV_{RAP}. For this reason, more work is needed into more robust methods for deriving beat-to-beat values of RAP and CrCP. One possibility, which remains to be investigated, is the alternative model proposed by Varsos *et al*, based on the concept of arterial impedance (Varsos *et al.* 2013).

The rejection of 44 subjects was also directly dependent on the confidence levels adopted for the coherence function in the frequency interval 0.15–0.25 Hz. Compared to the more classical estimates of the MAP–CBFV relationship, this relatively high number of cases with low coherence was likely to result from the difficulty of obtaining accurate estimates of CrCP and RAP for each cardiac cycle (Panerai *et al.* 2011). As described previously (Panerai *et al.* 2016), the reasoning for adopting the 0.15–0.25 Hz frequency interval was to avoid the frequency region where dynamic CA is more likely to be non-linear (<0.15 Hz), but still maintain an acceptable signal-to-noise ratio (<0.25 Hz). Although initially derived for the MAP–CBFV relationship, from a statistical standpoint, the criterion based on confidence limits also applies to any transfer function since it is based on the use of random noise for the input and output functions (Claassen *et al.* 2016). A problem exists, though, when the criterion is applied to multiple transfer functions, as was our case. The 95% confidence limit for the mean coherence function in the range 0.15–0.25 Hz that we found in previous studies was approximately 0.190 when using 5 min recordings, with five segments of 102.4 s duration and 50% superposition (Claassen *et al.* 2016; Panerai *et al.* 2016, 2018). However, when applying this approach to multiple transfer functions, also subjected to the condition that it must be satisfied for both normocapnia and hypercapnia, the 95% limit is likely to be much lower and further studies of this joint distribution would be needed. In the absence of this information, we adopted the 90% confidence limit of 0.150 as a very conservative threshold for acceptance of the SRV_{RAP} and SRV_{CrCP}. With more in-depth studies of the joint distribution of coherence for multiple SR, it is very likely that the number of subjects yielding acceptable estimates of SRV_{CrCP} and SRV_{RAP} will increase significantly. Nevertheless, as mentioned above, dismissing the 95% confidence criterion for coherence, and re-analysing the data with all 120 subjects included, did not show any significant differences in the main conclusions of the study.

Physiological interpretation

The temporal pattern of SRV_{RAP} fits well with established concepts about the myogenic response of intra-cerebral vessels to a sudden change in MAP (Panerai *et al.* 2006, 2011). What is novel, and puzzling, is the corresponding temporal pattern of SRV_{CrCP}. A sudden increase in MAP leads to alterations in VSM membrane permeability to potassium and calcium, which will increase VSM contraction and thus reduce vessel diameter and blood flow (Faraci *et al.* 1989). With reduced arterial diameters

and stiffer vessel walls, CrCP will increase (Burton, 1951; Panerai, 2003), leading to the initial reduction in SRV_{CrCP}. CrCP is also influenced by ICP (Panerai, 2003), which tends to increase with hypercapnia (Hoiland *et al.* 2019). What is puzzling, though, is why SRV_{CrCP} then reaches a minimum and gradually increases continuously (Figs 1*C* and 2*C*). This behaviour of SRV_{CrCP}, approximately 3 s after the MAP change, has two main effects. First, it counteracts the continuous reduction in SRV_{RAP}, leading to relatively stable values of SRV_{MCA} during this phase of the responses. Second, it contributes to the much larger values of SRV_{MCA} observed during hypercapnia, when compared to the normocapnic response. At this stage, we can only speculate about the underlying physiological mechanisms responsible for the SRV_{CrCP} pattern. It is generally accepted that capillaries and pre-capillary arterioles are the vessels that could collapse at small values of transmural pressure, and for this reason they represent the segment of the cerebral circulation that would contribute to changes in CrCP. Increases in flow in small arterioles elicit the release of nitric oxide by the endothelium, due to the phenomenon of shear stress, leading to vasodilatation (Hoiland *et al.* 2019). However, the response to changes in shear stress involves a time delay, which can be up to 30 s, but if shorter, or mediated by more rapid neurotransmitters, would fit well with the slow rise in SRV_{CrCP} observed in Figs 1*C* and 2*C*. The finding that SRV_{CrCP} reached more positive values during hypercapnia (Figs 1*C* and 2*C*), reinforces this interpretation, due to the more pronounced effects of shear stress that have been associated with hypercapnia (Hoiland *et al.* 2019). More work is needed to shed light on the determinants of the CrCP response to a step change in MAP. Changes in posture, which can alter intracranial pressure, or neural stimulation, which can also lead to vasodilatation of small arterioles, would be two interesting possibilities to be tested. Independently of the mechanistic factors determining the gradual rise in CRV_{CrCP} in the late phase of the response, our findings confirmed the strong sensitivity of CrCP to P_{aCO_2} (Table 1) that has been previously reported by several studies (Panerai, 2003). This association, together with the CrCP response to neural stimulation (Panerai *et al.* 2005, 2012; Beishon *et al.* 2018) has led to speculations that whilst RAP might be more sensitive to vessel diameter changes due to myogenic mechanisms (Salinet *et al.* 2013; van Veen *et al.* 2015), CrCP might be more responsive to vasomotor activity of metabolic origin.

Limitations of the study

Several important limitations of the study were addressed above, including the rejection of 44 subjects due to the low coherence in either the V_{MAP}–V_{RAP} or V_{MAP}–V_{CrCP} transfer functions.

As with any studies based on TCD, attention is needed to factors that could influence MCA diameter, with consequent disruption of a stable relationship between CBFV and absolute CBF. Hypercapnia has been shown to increase MCA diameter (Coverdale *et al.* 2014; Verbree *et al.* 2014), but only at levels of P_{aCO_2} much higher than those inferred from our measurements of ET_{CO_2} (Table 1). Nevertheless, if we accept that minor vasodilatation of the MCA might have led to CBFV underestimating CBF, any effects in our results would be minimised by the normalisation procedure inherent to SCA (Appendix).

Although the levels of ET_{CO_2} attained due to breathing of 5% CO_2 in air were significantly higher than those recorded during normocapnia at baseline (Table 1), when compared to the majority of studies in the literature, they should be regarded as mild hypercapnia. The relatively low values of ET_{CO_2} that we obtained were the result of two limitations. First, participants breathed 5% CO_2 in air at their own respiratory frequency and tidal volume. Much higher values of P_{aCO_2} could be achieved with the use of a computerised closed-loop end-tidal forcing system, using a higher target for ET_{CO_2} (Hoiland *et al.* 2019). Second, 5% CO_2 breathing took place for 3 min and hence its effects were diluted within recordings lasting a total of 5 min, both for its mean values (Table 1) and for the TFA and resultant estimates of SRs. The other side of this limitation, though, is that our relatively low values of ET_{CO_2} during hypercapnia were well below the levels where dilatation of the MCA would have raised concerns about underestimation of changes in CBF (Coverdale *et al.* 2014; Verbree *et al.* 2014). In addition, despite only mild hypercapnia being achieved, we still detected highly significant effects of P_{aCO_2} on SRV_{CrCP} and it is open to question whether similar or even stronger effects would be obtained with higher levels of P_{aCO_2}. On the other hand, it is possible that with wider changes in P_{aCO_2} the RAP step responses might show significant differences, due to hypercapnia or hypocapnia, contrary to our results in Tables 1 and Figs 1–3.

In this study, dynamic CA was probed by spontaneous fluctuations in MAP, but the reliability of this approach has been questioned, due to the relatively low amplitude of MAP changes observed with spontaneous variability, in comparison with alternative approaches such as the rapid release of pressurised thigh cuffs or repeated squat–stand manoeuvres (Aaslid *et al.* 1989; Claassen *et al.* 2009; Simpson & Claassen, 2018). On the other hand, spontaneous MAP variability affords minimal disruption to underlying physiological processes and it can be adopted in most clinical studies (Tzeng & Panerai, 2018). Nevertheless, further studies of the SRV_{CrCP} and SRV_{RAP} with different protocols to induce larger changes in MAP would be of considerable interest, to provide a better understanding of the influences of co-factors, such as sympathetic activation (Tzeng & Panerai, 2018), and to test the linearity of the responses to larger changes in MAP.

The linear model linking CrCP and RAP to mean values of CBFV and BP for each cardiac cycle, as expressed by eqns (A2)–(A10) (Appendix) relies on a number of assumptions whose limitations need to be kept in mind. Firstly, for a single cardiac cycle, it is unlikely that the assumption of a linear instantaneous relationship between CBFV and BP would hold at very low values of diastolic BP, leading to the distinction between 'true' and 'apparent' CrCP (Panerai, 2003). However, the linear relationship has been shown to represent an acceptable model in the physiological range of diastolic BP values (Panerai, 2003; Panerai *et al.* 2011), but that might not be the case in the presence of severe arterial hypotension. Secondly, as also expressed by eqns (A2)–(A10), the interdependence between beat-to-beat values of CBFV, MAP, RAP and CrCP means that of these four parameters, only three are independent, and this is also the case of the relationship between the corresponding step responses. In this study, this interdependence was circumvented by obtaining separate estimates of the V_{MAP}–V_{CBFV}, V_{MAP}–V_{RAP} and V_{MAP}–V_{CrCP} step responses, thus leaving the fourth parameter, i.e. V_{MAP}, as the dependent variable in eqns (A2)–(A10), only used to confirm the numerical accuracy of the three distinct transfer function calculations, as the 'checksum' illustrated in Fig. 1*D*. As a result of this approach, our estimates of SRV_{RAP} and SRV_{CrCP} can be considered as independent of each other, as demonstrated by the distinct temporal patterns in Figs 1 and 2.

Finally, we have not considered the potential effects of sex or age on estimates of SR_{RAP} and SR_{CrCP}. This would be worth investigating, given previous indications that RAP increases with ageing and the non-linear dependence of RAP and CrCP on P_{aCO_2} is influenced by sex (Minhas *et al.* 2018*b*, 2019).

Conclusions

In a relatively large number of healthy subjects, the use of TFA for assessment of dynamic CA was extended to include the separate contributions of RAP and CrCP to explain the temporal pattern of the CBFV response to a step change in MAP. Of considerable relevance, the contribution of CrCP to the CBFV step response was not only highly significant during normocapnia at rest, but during hypercapnia it became the dominant factor to explain the changes in the CBFV response, without a contribution from RAP. These findings could have considerable impact on future studies of dynamic CA in humans, but further work is needed to confirm their generalizability to different populations and the extent to which the increase in the dimensionality of CA assessment, afforded by the separate analysis of the RAP and CrCP contributions, could improve the sensitivity and specificity of clinical applications.

Appendix

Sub-component analysis

For each cardiac cycle, the instantaneous relationship between arterial blood pressure (BP) and cerebral blood flow velocity (CBFV) can be approximated by (Panerai, 2003):

$$v_i(t) = \frac{p_i(t) - CrCP_i}{RAP_i} \quad (A1)$$

where $v_i(t)$ and $p_i(t)$ are the instantaneous CBFV and BP for the ith cardiac cycle and $CrCP_i$ and RAP_i are the corresponding critical closing pressure and resistance–area product parameters obtained by fitting a linear relationship (Panerai *et al.* 2011). When averaged over the entire cardiac cycle, or a longer period, eqn (A1) can be expressed as:

$$V_i = \frac{MAP_i - CrCP_i}{RAP_i} \quad (A2)$$

where V_i represents the mean value of $v_i(t)$ for the cardiac cycle and MAP_i is the corresponding mean of $p_i(t)$.

When MAP_i changes from its mean value by an amount Δp, it will induce changes in V_i as well as changes in $CrCP_i$ and RAP_i, leading to:

$$V_i + \Delta v = \frac{(MAP_i + \Delta p) - (CrCP_i + \Delta c)}{RAP_i + \Delta r} \quad (A3)$$

where Δv, Δc and Δr represent small changes in V_i, $CrCP_i$ and RAP_i, respectively.

Assuming that $\Delta r << RAP$

$$\frac{1}{RAP_i + \Delta r} \approx \frac{1}{RAP_i}\left(1 - \frac{\Delta r}{RAP_i}\right) \quad (A4)$$

Substituting in (A3):

$$V_i + \Delta v \approx (MAP_i + \Delta p - CrCP_i - \Delta c)$$
$$\times \frac{1}{RAP_i}\left(1 - \frac{\Delta r}{RAP_i}\right) \quad (A5)$$

Neglecting second order products ($\Delta r.\Delta p \approx 0$ and $\Delta r.\Delta c \approx 0$) and using eqn (A1):

$$V_{MCA} = \frac{1}{RAP_i}(\Delta p - \Delta c - \Delta r.V_i) \quad (A6)$$

where $V_{MCA} \approx \Delta v$.

Defining:

$$V_{MAP} = \frac{\Delta p}{RAP_i} \quad (A7)$$

$$V_{CrCP} = -\frac{\Delta c}{RAP_i} \quad (A8)$$

$$V_{RAP} = -\frac{\Delta r.V_i}{RAP_i} \quad (A9)$$

with the result

$$V_{MCA} = V_{MAP} + V_{CrCP} + V_{RAP} \qquad (A10)$$

and the total change in CBFV, V_{MCA}, is now approximated as the sum of three sub-components, reflecting the separate contributions of parallel changes in MAP, CrCP and RAP. The great advantage of eq. (A10) is that each sub-component has the same units of CBFV (cm s^{-1}). In other words, the transformations expressed by eqns (A1–A10) allow us to have a uniform 'currency' to compare different contributions to changes in CBFV.

References

Aaslid R, Lindegaard KF, Sorteberg W & Nornes H (1989). Cerebral autoregulation dynamics in humans. *Stroke* **20**, 45–52.

Beishon LC, Williams CAL, Robinson TG, Haunton VJ & Panerai RB (2018). Neurovascular coupling response to cognitive examination in healthy controls: a multivariate analysis. *Physiol Rep* **6**, e13803.

Bendat JS & Piersol AG (1986). *Random Data Analysis and Measurement Procedures.* John Wiley & Sons, New York.

Burton AC (1951). On the physical equilibrium of small blood vessels. *Am J Physiol* **164**, 319–329.

Castro P, Santos R, Freitas J, Panerai RB & Azevedo E (2014). Autonomic dysfunction affects dynamic cerebral autoregulation during Valsalva maneuver: comparison between healthy and autonomic dysfunction subjects. *J Appl Physiol* **117**, 205–213.

Claassen JAHR, Levine BD & Zhang R (2009). Dynamic cerebral autoregulation during repeated squat-stand maneuvers. *J Appl Physiol* **106**, 153–160.

Claassen JAHR, Meel-van den Abeelen ASS, Simpson DM & Panerai RB (2016). Transfer function analysis of dynamic cerebral autoregulation: a white paper from the International Autoregulation Research Network (CARNet). *J Cereb Blood Flow Metab* **36**, 665–680.

Coverdale NS, Gati JS, Opalevych O, Perrotta A & Shoemaker JK (2014). Cerebral blood flow velocity underestimates cerebral blood flow during models hypercapnia and hypocapnia. *J Appl Physiol* **117**, 1090–1096.

Czosnyka M, Brady K, Reinhard M, Smieleswski P & Steiner LA (2009). Monitoring of cerebrovascular autoregulation: Facts, myths, and missing links. *Neurocrit Care* **10**, 373–386.

Czosnyka M, Smielewski P, Kirkpatrick P, Laing RJ, Menon D & Pickard JD (1997). Continuous assessment of the cerebral vasomotor reactivity in head injury. *Neurosurgery* **41**, 11–19.

Czosnyka M, Smielewski P, Kirkpatrick P, Menon DK & Pickard JD (1996). Monitoring of cerebral autoregulation in head-injured patients. *Stroke* **27**, 1829–1834.

Edwards MR, Devitt DL & Hughson RL (2004). Two-breadth CO$_2$ test detects altered dynamic cerebrovascular autoregulation and CO$_2$ responsiveness with changes in arterial PCO$_2$. *Am J Physiol Regul Integ Comp Physiol* **287**, R627–R632.

Edwards MR, Shoemaker JK & Hughson RL (2002). Dynamic modulation of cerebrovascular resistance as an index of autoregulation under tilt and controlled PETCO$_2$. *Am J Physiol Reg Integr Comp Physiol* **283**, R653–R662.

Elting JW, Maurits NM & Aries MJH (2014). Variability of the autoregulation index decreases after removing the effect of the very low frequency band. *Med Eng Phys* **36**, 601–606.

Evans DH, Levene MI, Shortland DB & Archer LN (1988). Resistance index, blood flow velocity, and resistance area product in the cerebral arteries of very low birth weight infants during the first week of life. *Ultrasound Med Biol* **14**, 103–110.

Faraci FM, Baumbach GL & Heistad DD (1989). Myogenic mechanisms in the cerebral circulation. *J Hypertension* **7**, S61–S64.

Garnham J, Panerai RB, Naylor AR & Evans DH (1999). Cerebrovascular response to dynamic changes in pCO$_2$. *Cerebrovasc Dis* **9**, 146–151.

Hoiland RL, Fisher JA & Ainslie PN (2019). Regulation of the cerebral circulation by arterial carbon dioxide. *Compr Physiol* **9**, 1101–1154.

Hughson RL, Edwards MR, O'Leary DD & Shoemaker JK (2001). Critical analysis of cerebrovascular autoregulation during repeated head-up tilt. *Stroke* **32**, 2403–2408.

Intharakham K, Beishon LC, Panerai RB, Haunton VJ & Robinson TG (2019). Assessment of cerebral autoregulation in stroke: a systematic review and meta-analysis of studies at rest. *J Cereb Blood Flow Metab* **39**, 2105–2116.

Katsogridakis E, Bush G, Fan L, Birch AA, Simpson DM, Allen R, Potter JF & Panerai RB (2013). Detection of impaired cerebral autoregulation improves by increasing arterial blood pressure variability. *J Cereb Blood Flow Metab* **33**, 519–523.

Liu J, Simpson DM & Allen R (2005). High spontaneous fluctuations in arterial blood pressure improves the assessment of cerebral autoregulation. *Physiol Meas* **26**, 725–741.

Llwyd O, Panerai RB & Robinson TG (2017). Effects of dominant and non-dominant passive arm manoeuvres on the neurovascular coupling response. *Eur J Applied Physiol* **117**, 2191–2199.

Maggio P, Salinet ASM, Panerai RB & Robinson TG (2013). Does hypercapnia-induced impairment of cerebral autoregulation affect neurovascular coupling? A functional TCD study. *J Appl Physiol* **115**, 491–497.

Marmarelis VZ, Shin DC, Orme M & Zhang R (2014). Time-varying modeling of cerebral hemodynamics. *IEEE Trans Biomed Eng* **61**, 694–704.

Minhas JS, Haunton VJ, Robinson TG & Panerai RB (2019). Determining differences between critical closing pressure and resistance-area product: responses of the healthy young and old to hypocapnia. *Eur J Physiol* **471**, 1117–1126.

Minhas JS, Panerai RB & Robinson TG (2018*a*). Modelling the cerebral haemodynamic response in the physiological range of PaCO$_2$. *Physiol Meas* **39**, 1–11.

Minhas JS, Panerai RB & Robinson TG (2018*b*). Sex differences in cerebral haemodynamics across the physiological range of PaCO$_2$. *Physiol Meas* **39**, 105009.

Murkin JM (2007). Cerebral autoregulation: The role of CO_2 in metabolic homeostasis. *Seminars in Cardiothor Vasc Anesth* **11** 269–273.

O'Leary DD, Shoemaker JK, Edwards MR & Hughson RL (2004). Spontaneous beat-by-beat fluctuations of total peripheral and cerebrovascular resistance in response to tilt. *Am J Physiol Regul Integr Comp Physiol* **287**, R670-R679.

Panerai RB (1998). Assessment of cerebral pressure autoregulation in humans – a review of measurement methods. *Physiol Meas* **19**, 305–338.

Panerai RB (2003). The critical closing pressure of the cerebral circulation. *Med Eng Phys* **25**, 621–632.

Panerai RB (2008). Cerebral autoregulation: From models to clinical applications. *Cardiovasc Eng* **8**, 42–59.

Panerai RB, Dawson SL, Eames PJ & Potter JF (2001). Cerebral blood flow velocity response to induced and spontaneous sudden changes in arterial blood pressure. *Am J Physiol Heart Circ Physiol* **280**, H2162-H2174.

Panerai RB, Deverson ST, Mahony P, Hayes P & Evans DH (1999). Effect of CO_2 on dynamic cerebral autoregulation measurement. *Physiol Meas* **20**, 265–275.

Panerai RB, Eames PJ & Potter JF (2006). Multiple coherence of cerebral blood flow velocity in humans. *Am J Physiol Heart Circ Physiol* **291**, H251–H259.

Panerai RB, Eyre M & Potter JF (2012). Multivariate modeling of cognitive-motor stimulation on neurovascular coupling: transcranial Doppler used to characterize myogenic and metabolic influences. *Am J Physiol Regul Integr Comp Physiol* **303**, R395–R407.

Panerai RB, Haunton VJ, Minhas JS & Robinson TG (2018). Inter-subject analysis of transfer function coherence in studies of dynamic cerebral autoregulation. *Physiol Meas* **39**, 125006.

Panerai RB, Haunton VJ, Salinet ASM & Robinson TG (2016). Statistical criteria for estimation of the cerebral autoregulation index (ARI) at rest. *Physiol Meas* **37**, 661–672.

Panerai RB, Moody M, Eames PJ & Potter JF (2005). Cerebral blood flow velocity during mental activation: Interpretation with different models of the passive pressure-velocity relationship. *J Appl Physiol* **99**, 2352–2362.

Panerai RB, Rennie JM, Kelsall AWR & Evans DH (1998*a*). Frequency-domain analysis of cerebral autoregulation from spontaneous fluctuations in arterial blood pressure. *Med Biol Eng Comput* **36**, 315–322.

Panerai RB, Robinson TG & Minhas JS (2019). The upper frequency limit of dynamic cerebral autoregulation. *J Physiol* **597**, 5821–5833.

Panerai RB, Salinet ASM, Brodie FG & Robinson TG (2011). The influence of calculation method on estimates of cerebral critical closing pressure. *Physiol Meas* **32**, 467–482.

Panerai RB, White RP, Markus HS & Evans DH (1998*b*). Grading of cerebral dynamic autoregulation from spontaneous fluctuations in arterial blood pressure. *Stroke* **29**, 2341–2346.

Patel N, Panerai RB, Haunton VJ, Katsogridakis E, Saeed NP, Salinet ASM, Brodie FG, Syed N, D'Sa S & Robinson TG (2016). The Leicester cerebral haemodynamics database: normative values and the influence of age and sex. *Physiol Meas* **37**, 1485–1498.

Salinet ASM, Robinson TG & Panerai RB (2013). Cerebral blood flow response to neural activation after acute ischemic stroke: a failure of myogenic autoregulation? *J Neurol* **260**, 2588–2595.

Simpson DM & Claassen J (2018). CrossTalk opposing view: dynamic cerebral autoregulation should be quantified using induced (rather than spontaneous) blood pressure fluctuations. *J Physiol* **596**, 7–9.

Tiecks FP, Lam AM, Aaslid R & Newell DW (1995). Comparison of static and dynamic cerebral autoregulation measurements. *Stroke* **26**, 1014–1019.

Tzeng YC, Ainslie PN, Cooke WH, Peebles KC, Willie CK, MacRae BA, Smirl JD, Horsman HM & Rickards CA (2012). Assessment of cerebral autoregulation: the quandary of quantification. *Am J Physiol Heart Circ Physiol* **303**, H658–H671.

Tzeng YC & Panerai RB (2018). CrossTalk proposal: dynamic cerebral autoregulation should be quantified using spontaneous blood pressure fluctuations. *J Physiol* **596**, 3–5.

van Beek AHEA, Claassen JAHR, Rikkert O & Jansen RWMM (2008). Cerebral autoregulation: An overview of current concepts and methodology with special focus on the elderly. *J Cereb Blood Flow Metab* **28**, 1071–1085.

van Veen T, Panerai RB, Haeri S, Zeeman GG & Belfort MA (2015). Effect of breath-holding on cerebrovascular hemodynamics in normal pregnancy and preeclampsia. *J Appl Physiol* **118**, 858–862.

Varsos GV, Richards H, Kasprowicz M, Budohoski KP, Brady KM, Reinhard M, Avolio A, Smieleswski P, Pickard JD & Czosnyka M (2013). Critical closing pressure determined with a model of cerebrovascular impedance. *J Cereb Blood Flow Metab* **33**, 235–243.

Verbree J, Bronzwaer ASGT, Ghariq E, Versluis MJ, Daemen MJAP, van Buchem MA, Dahan A, van Lieshout JJ & van Osch MJP (2014). Assessment of middle cerebral artery diameter during hypocapnia and hypercapnia in humans using ultra-high-field MRI. *J Appl Physiol* **117**, 1084–1089.

Welch PD (1967). The use of the Fast Fourier Transform for the estimation of power spectra: a method based on time averaging over short, modified periodograms. *IEEE Trans Audio Electroacoust* **15** 70–73.

Willie CK, Tzeng YC, Fisher JA & Ainslie PN (2014). Integrative regulation of human brain blood flow. *J Physiol* **592**, 841–859.

Zhang R, Zuckerman JH, Giller CA & Levine BD (1998). Transfer function analysis of dynamic cerebral autoregulation in humans. *Am J Physiol Heart Circ Physiol* **274**, H233-H241.

Additional information

Data availability statement

Supporting information

Additional supporting information may be found online in the Supporting Information section at the end of the article.

Statistical Summary Document